ENHANCED PHOTOCATALYTIC PROPERTIES OF MnOx CO-CATALYTIC MODIFIED ZnO NANOSTRUCTURED FILMS FOR ORGANIC DYE DEGRADATION

Dobrina Ivanova[1], Silviya Simeonova[2], Nina Kaneva[1]

[1]*Laboratory of Nanoparticle Science and Technology*
Department of General and Inorganic Chemistry
Faculty of Chemistry and Pharmacy, University of Sofia
Sofia 1164, Bulgaria
[2]*Laboratory of Atomic Force Microscopy*
Department of Physical Chemistry, Faculty of Chemistry and Pharmacy
University of Sofia, 1 James Bourchier Blvd., Sofia 1164, Bulgaria
E-mail: dobrina.k.ivanova@gmail.com

ABSTRACT

This work aims to enhance the photocatalytic activity of ZnO films for persistent organic pollutants. The photocatalysis method has gained significant interest as a sustainable and environmentally friendly approach to enhance the safety of clean water by eliminating persistent organic pollutants. Zinc oxide as a transition metal oxide is recognized as a highly effective material for photocatalysis. Even so, ZnO can be modified to increase its action and result in a more significant degradation of organic pollutants. In the photocatalytic process, an electron from the valence band is excited and moves to a higher energy level, the conduction band. Thus, an electron-hole pair is formed. Unstoichiometry transition metal oxides, such as MnOx are hole-trapping co-catalysts that promote oxidation processes.

This research reported the sol-gel synthesis of ZnO nanostructured films co-catalytic modified with MnOx for organic dye degradation. The confirmed features of ZnO/MnOx films are characterized by different analytical tools such as atomic force microscopy (AFM), X-ray diffraction analysis (XRD) and UV-Vis spectroscopy. The surface of the zinc oxide revealed a hexagonal wurtzite structure and a visible ganglia-like pattern. MnOx co-catalytic modification plays a vital role in the percent degradation of the organic dye under UV-irradiation conditions.

Keywords: ZnO/MnOx, co-catalytic modification, UV, sol-gel films, Reactive Black 5.

INNTRODUCTION

Zinc oxide is inexpensive, non-toxic, chemically stable, easy to prepare, reproducible and most of the modifying materials used with it, also readily available and become more efficient. It has various applications, such as solar cell, photoelectric cells, nonlinear optics [1 - 3] and micro-gas sensing devices [4]. Furthermore, because of its transparency, ZnO is attractive for integrated photonic devices [5] and photocatalysts for wastewater treatment [6, 7]. ZnO thin films are prepared using various methods - reactive sputtering [8], spray pyrolysis [9], electrodeposition [10], chemical vapor deposition [11], magnetron sputtering [12], chemical bath deposition [13], sol-gel [14, 15], etc. The sol-gel method has emerged as one of the most promising techniques, because it is particularly efficient in producing thin, transparent, homogeneous, multicomponent oxide films of many compositions on various substrates at low cost.

ZnO has a wide band gap (Eg = 3.28 - 3.32 eV [16]), which limits its photocatalytic effectiveness under ultraviolet illumination. Furthermore, the photocatalytic activity of a photocatalyst is closely dependent on the

recombination rate of the photogenerated electron-hole pairs [17]. Therefore, the challenge is to extend the photosensitization and to improve the separation of the e^-/h^+. A promising strategy for minimizing recombination losses, while simultaneously improving surface charge transfers, is through introduction of co-catalysts on the ZnO surface. It has been found in many studies that the amount of modifying element used affects the structural, optical and photocatalytic activities of the catalyst [18, 19]. The incorporation of a transition metal or transition metal oxide which can form heterojunctions with ZnO and selectively accumulate either of the photogenerated charge carriers, thus reducing the semiconductor band gap [20]. Therefore, the present investigation is focused on the co-catalytic modifying ZnO with MnOx, which is a transition metal with half-filled 3d orbitals ($[Ar]3d^5 4s^2$). S. Senthilkumaar et al. reported that doping ZnO with an optimum amount of Mn leads to a decrease in the band gap [21]. Manganese can also act as a trapper of charge carriers by generating isolated impurity energy levels in the band gap [22].

In this work, ZnO and ZnO/MnOx thin films are prepared using the sol-gel method, chemical deposition, and dip-coating technique. For the first time, we evaluated the photocatalytic activity of MnOx co-catalytic modified ZnO nanostructures photo-fixed with ultraviolet illumination at different doses of illumination ($2.5, 5, 10 \text{ J cm}^{-2}$). The structural properties are analyzed by X-ray diffraction (XRD). The morphology and elemental composition of the modified films are examined using Atomic Force Microscopy (AFM) and Energy Dispersive X-ray Spectroscopy (EDS). The optical properties are investigated using UV-Vis spectroscopy. The photocatalytic efficiency of pure and MnOx-modified ZnO nanomaterials are assessed using Reactive Black 5 (RB5) as a typical organic pollutant in an aqueous solution under UV irradiation.

EXPERIMENTAL

Zinc acetate dehydrate (> 99.9 %) was obtained from Sigma-Aldrich. Monoethanolamine and 2 methoxyethanol (> 99.9 %) - from Fluka. Manganese (II) sulfate (> 99 %) and Potassium iodate (> 99.5 %) were from Sigma-Aldrich. All chemicals were of analytical reagent grade and without further purification. The glass substrates (ca. 76 mm × 26 mm, ISO-LAB,) are used as substrates.

Reactive Black 5 ($C_{26}H_{21}N_5Na_4O_{19}S_6$, $\lambda_{max} = 595$ nm, dye content ca. 55 % from Sigma–Aldrich) was chosen as a typical organic pollutant for the photocatalytic experiments. The reason is his large-scale application in practice - textile industries for cotton, viscose, wool, and polyamide fabric dyeing. It is also used as a staining dye in clinical laboratories for cell biology, hematology, and history research. RB5 may cause allergies, asthma symptoms, or breathing difficulties, as pointed out by the supplier. Distilled water was used for the experiments to prove the photocatalytic degradation of Reactive Black 5 in the presence of ZnO and ZnO/MnOx, photo-fixed with UV light at different doses of irradiation.

In this study, pure and MnOx-modified ZnO films were prepared using a sol-gel method. Briefly, to prepare ZnO thin films, zinc acetate dehydrate was dissolved in 2-methoxyethanol under constant stirring at room temperature. After that, monoethanolamine was added dropwise to the solution. The precursor sol was kept under magnetic stirring for 1 h at 60°C to obtain a homogenous and clear color. The solution was aged 24 h and then was used for depositing over glass substrates by means of a dip-coating technique. After that, the samples were dried at 100°C for 10 min to evaporate the organic residual material. The pure sol-gel films had 5 coats. Finally, nanostructure samples were annealed at 500°C for 1 h in the oven.

MnOx solution was obtained as the aqueous solution (5 mM precursor ion content) of Mn^{2+} was added to an equimolar electron scavenger (IO_3^-). ZnO/MnOx sol-gel films were received by chemical photo-deposition in three steps: (i) pure ZnO films were immersed in an as-prepared MnOx solution with 10^{-2} M concentration, (ii) photo-fixed with UV light at different doses of illumination ($2.5, 5$ and 10 J cm^{-2}), (iii) after the photo-fixation. The three types ZnO/MnOx samples were washed with water and dried at 100 °C for 10 minutes.

AFM imaging was performed on the NanoScope V system (Bruker Ltd, Germany) operating in tapping mode in the air at room temperature. Silicon cantilevers (Tap 300Al-G, Budget Sensors, Innovative Solutions Ltd, Bulgaria) with 30 nm thick aluminum reflex coatings were used. According to the producer's datasheet, the cantilever force constant and the resonance frequencies are in the range of 40 N/m and 300 kHz, respectively. The tip radius was less than 10 nm. The scan rate was set at 1 Hz and the images were captured in height mode with

512×512 pixels in JEPG. Subsequently, all images were flattened using NanoScope software. The same software was also used for section and roughness analysis.

X-ray diffraction (XRD) was used to confirm the purity and the crystalline of the as prepared films using a Siemens D500 with CuKα radiation within 2θ range 30 - 70° at a step of 0.05° *2θ* and counting time 2 s/step.

The optical properties were investigated using UV-Vis spectroscopy by Evaluation 300 Thermo Scientific spectrophotometer. The obtained absorption data were converted to estimate the band gap energies (Eg) by applying the Tauc's formula *(αhν)ⁿ = A(hν–Eg)* [23], where *A* is a constant of proportionality, *α* is the linear absorption constant, *h* is the Planck's constant, and *n* = 2, assuming an indirect band gap transition for ZnO materials [23].

The photocatalytic tests were conducted in glass reactor, equipped with magnetic stirrer and UV lamp (36 W). The assays were performed at room temperature and at a constant stirring rate of 500 rpm.

The photocatalytic activity of ZnO and ZnO/MnOx films was compared in the degradation of Reactive Black 5. The volume of the pollutant solution was 150 ml with an initial concentration of 5 mg/L. The degradation process of the dye was measured by UV-Vis absorbance spectroscopy (spectrophotometer Evolution 300 Thermo Scientific, wavelength range from 400 to 800 nm) at room temperature under UV illumination.

The degree (*D* (%)) of photocatalytic degradation of Reactive Black 5 was calculated using the equation:

$$D\% = (C_o - C_t)/C_o.100 \qquad (1)$$

where C_o represents the initial concentration, C_t represents the drug concentration after *t* min of photocatalysis.

RESULTS AND DISCUSSION

The sectional analysis (scanned area 5×5 μm) of the surface of the samples, as and ganglia-like structures with height in the interval from 500 nm to 250 nm for ZnO/MnOx sol-gel films, photo-fixed with ultraviolet light at different UV doses 2.5 J cm⁻², 5 J cm⁻² and 10 J cm⁻² are shown in Fig. 1. The roughness values for the ZnO/MnOX samples are close, but the roughness of the modified films at UV dose 10 J cm⁻² is the lowest (Rq = 243 nm, Ra = 191 nm). The largest roughness is observed in the nanostructures that are irradiated with the lowest dose of UV light (Rq = 280 nm, Ra = 231 nm). Surface morphology has a key impact on the degradation of organic pollutants found in polluted waters. Therefore, the nanostructure samples that have the most developed surface (roughness) are expected to have the highest photocatalytic efficiency and to degrade the dye most fast.

The elemental analysis is investigated using energy dispersive spectroscopy (Fig. 2). The EDS analyses indicate the presence of Zn, O, and Mn, confirming the absence of external impurities in the prepared solid. On the other hand, the elemental chemical composition obtained in the ZnO/MnOx sample shows (60.07 wt. % Zn, 39.21 wt. % O, and 0.72 wt. % Mn).

The X-ray pattern of ZnO/MnOx film is in concordance with the characteristic peaks of zinc oxide with a hexagonal wurtzite structure (Fig. 3). The peaks are indexed with a JCPDS card (No.96-230-0117), which corresponded to the (100), (002), (101), (110) and (201)
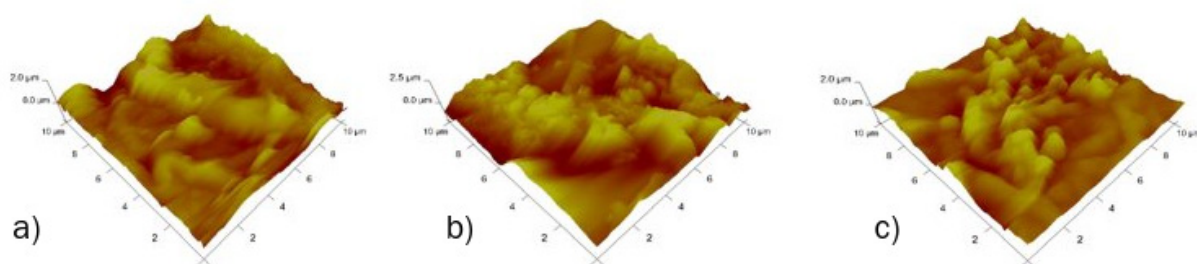

Fig. 1. Three dimensional AFM of the surface of ZnO/MnOx, photo-fixed with UV light at different doses of illumination: (a) 2.5 J cm⁻², (b) 5 J cm⁻², (c) 10 J cm⁻².
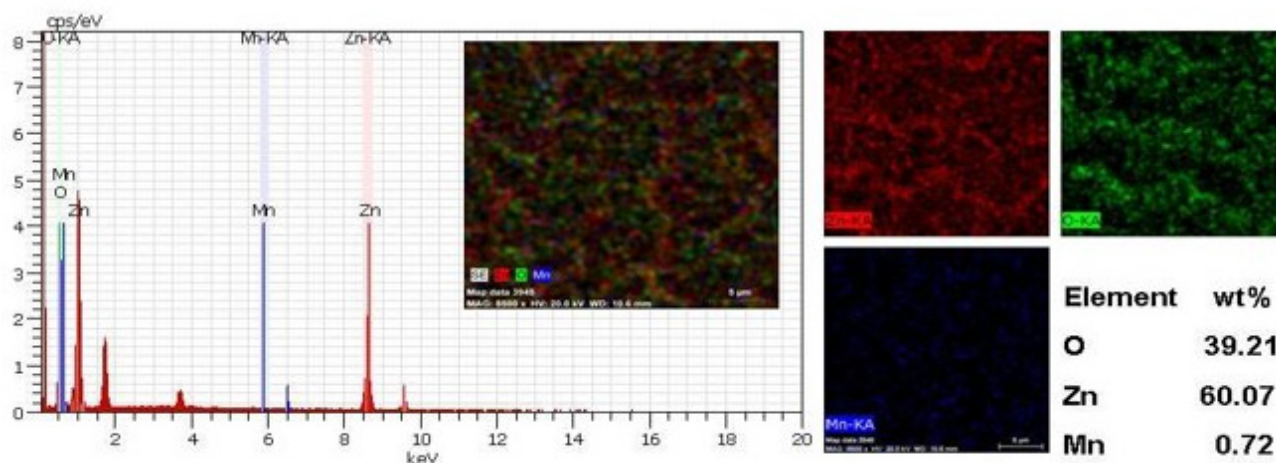
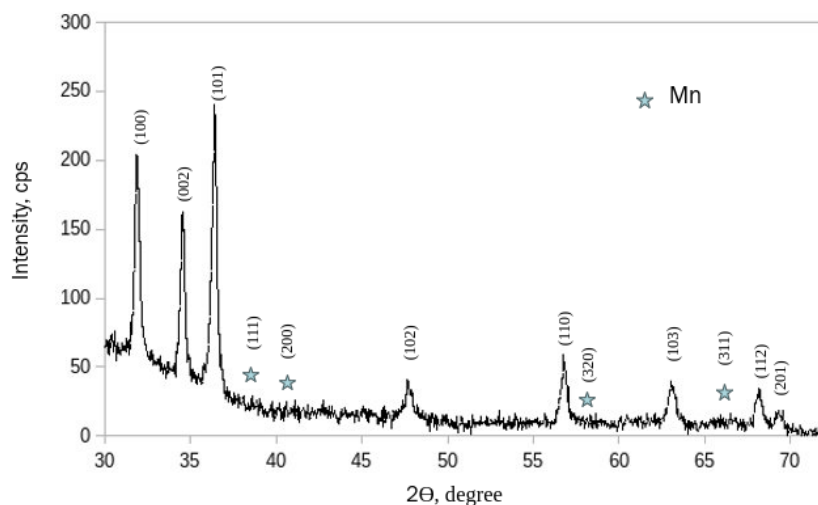Fig. 2. EDS spectra of MnOx co-catalytic modified ZnO film.

Fig. 3. XRD patterns of MnOx co-catalytic modified ZnO film.

planes. The diffraction peaks are sharp, indicating the high crystallinity of the material produced. However, when manganese is presented with a concentration of 10^{-2} M, additional peaks correspond to the planes (111, 200, 220, and 311) of the ionic form of Mn^{2+} (JCPDS 96-900-6670). The ionic radius of Mn^{2+} (0.80Å) is larger than that of Zn^{2+} (0.74Å), and no significant distortion in the lattice structure is observed. No impurity phase at tributes to manganese oxides could be detected, indicating that Mn^{2+} was completely modified onto the ZnO crystal lattice.

The optical properties of pure and Mn co-catalytic modified ZnO samples are further analyzed using UV-Vis spectroscopy (Fig. 4). Zinc oxide shows maximum absorption at 361 nm due to its band gap of 3.28 eV. After Mn^{2+} modifying of ZnO samples, the absorption increases (Fig. 4(a)). The band gap values were determined from UV-Vis spectra by converting the absorption to the Kubelka-Munk function and are found to decrease from 3.28 for ZnO to 3.25 eV for ZnO/MnOX, (Fig. 4(b)). Therefore, this indicates that the e^-/h^+ recombination is completely inhibited through the Mn^{2+} co-catalytic modification and the presence of a large number of carrier traps within the nanoparticles.
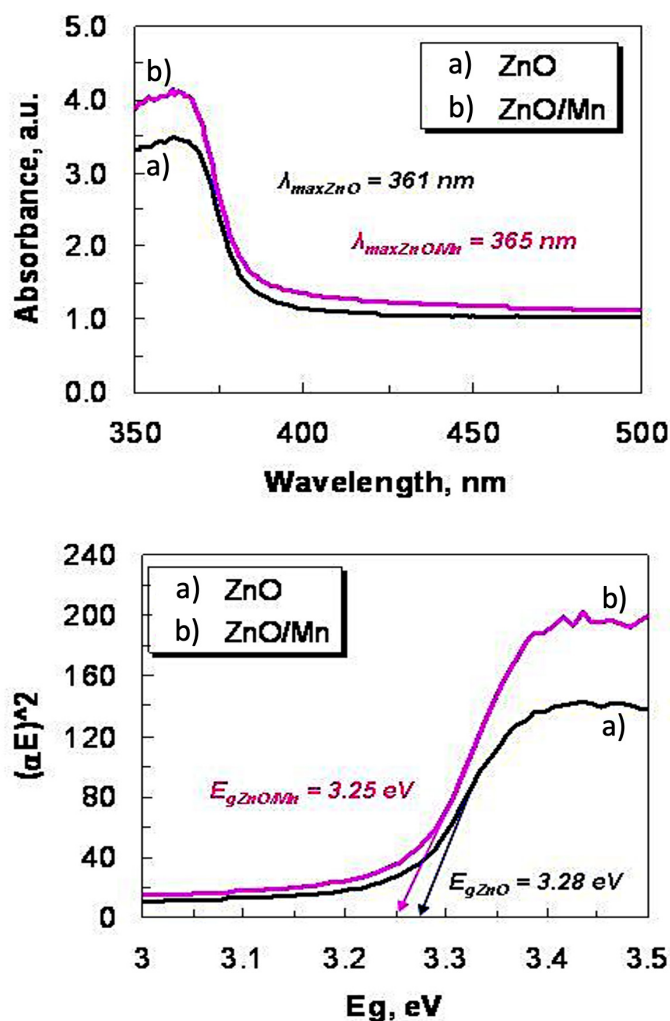
Fig. 4. Absorption spectrum (a) and Band gap (b) energy of ZnO and ZnO/MnOx sol-gel films.

This is one of the reasons why modified sol-gel films possess higher photocatalytic activity compared to pure zinc oxide.

The photocatalytic performance of the prepared nanostructure films is assessed under ultraviolet light irradiation using Reactive Black 5 (RB5) as a model dye. The obtained results are shown in Fig. 5. The rate constants k are estimated from the slopes of the linear plots of $Ln(C/C_o)$ versus irradiation time (Fig. 5(a)). The results indicate that the photocatalytic degradation of the dye with the pure and ZnO/MnOx, photo-fixed at different UV doses, are pseudo-first-order reactions in agreement

with a generally observed Langmuir–Hinshelwood mechanism [24]. The experimental results show that the rate constant for ZnO/MnOx (k = 0.4618 h^{-1}) is about 1.4 times higher than that of pure ZnO (k = 0.3283 h^{-1}). On the other hand, Fig. 5(b) shows the RB5 removal curves as a function of irradiation time under ultraviolet illumination. The pure ZnO film exhibited the lowest photocatalytic activity (D % = 69.79 %, calculated using Eq. 1). This behavior is expected, as the optical results showed that pure zinc oxide has a wider band gap (Eg = 3.28 eV). The modification with Mn^{2+} improved the photocatalytic performance of ZnO because decreasing
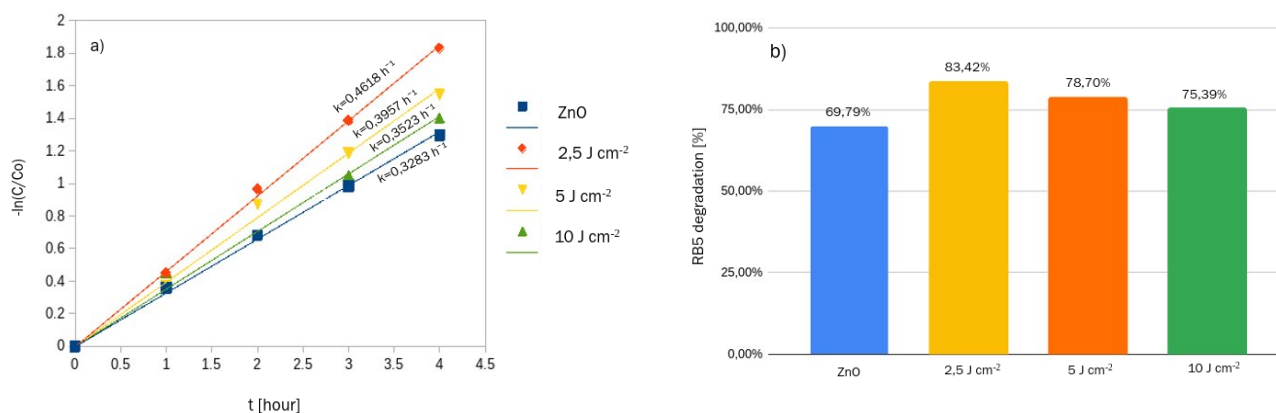
347

Fig. 5. Photocatalytic degradation of Reactive Black 5, using nanostructure films - ZnO and ZnO/MnOx, photo-fixed with UV illumination at different UV doses - 2.5, 5 and 10 J cm^{-2}.

in E_g for the ZnO/MnOx photocatalysts. These results are in agreement with the AFM results since they show that they have the most developed surface. It should be noted that the Mn co-catalytic modification of ZnO improved the RB5 degradation, leading to an almost complete elimination of the dye under UV irradiation ($D_{ZnO/MnOx}$ = 83.42 % at 2.5 J cm^{-2}; $D_{ZnO/MnOx}$ = 78.70 % at 5 J cm^{-2} and $D_{ZnO/MnOx}$ = 83.42 % at 10 J cm^{-2}). Our results are comparable to those reported by several authors [25, 26], who reported that ZnO doped with manganese exhibited a better photocatalytic performance compared to pure zinc oxide. Therefore, ZnO nanostructures modified by manganese nanostructures are promising and efficient catalysts for the decomposition of organic pollutants by photocatalytic oxidation.

CONCLUSIONS

In this work, pure and modified ZnO nanostructures are successfully synthesized using a sol-gel method and dip-coating technique. The films modified with manganese are carried out by photo-fixation with ultraviolet light at different UV doses, for the first time. The influence of the Mn^{2+} and UV dose of the photo-fixation on the structural, optical and photocatalytic properties of ZnO:Mn samples are investigated. ZnO/MnO$_x$ (UV dose = 2.5 J cm^{-2}) exhibit the highest photocatalytic efficiency for the degradation of Reactive Black 5 under ultraviolet illumination. This material also exhibits a higher developed surface (roughness) and decreases in the E_g than pure ZnO.

The manganese acts as an electron trap and decreases the photogenerated e$^-$/h$^+$ pair recombination resulting in an increase of the hydroxyl radicals by the ZnO/MnOx films and thus of its photocatalytic properties. The technique developed gives easy and fast access to Mn co-catalytic modified ZnO films (ZnO/MnOx) displaying high interest in environmental protection from organic pollutants.

REFERENCES

1. M. Tomar, V. Gupta, K. Sreenivas, A. Mansingh, Temperature stability of ZnO thin film SAW device on fused quartz, Dev. Mater. Res., 5, 3, 2005, 494-500.
2. S. Kodigala, 7 - Fabrication and Properties of Window Layers For Thin Film Solar Cells, Thin Films Nanostruct., 35, 2010, 393-504.
3. A. Kepceoglu, S. Gezgin, Y. Gundogdu, H. Kucukcelebi, H. Kilic, Nonlinear Optical Properties of Zinc Oxide Thin Films Produced by Pulsed Laser Deposition, Materialstoday: Proceed. 18, 5, 2019, 1819-1825.
4. Y. Hsiao, Y. Nagarjuna, G. Hung, M. Lin, Preparation of tungsten-doped zinc oxide thin films by co-sputtering for micro-gas sensing devices, J. Alloys Compd., 960, 2023, 170567.

5. B. Santoshkumar, S. Kalyanaraman, R. Vettumperumal, R. Thangavel, I. Kityk, S. Velumani, Structure-dependent anisotropy of the photoinduced optical nonlinearity in calcium doped ZnO nanorods grown by low-cost hydrothermal method for photonic device applications, J. Alloys Compd., 658, 2016, 435-439.

6. A. Colli, M. Fendrich, N. Bazzanella, Ch. Dridi, A. Miotello, M. Orlandi, Wastewater remediation with ZnO photocatalysts: Green synthesis and solar concentration as an economically and environmentally viable route to application, J. Environ. Manag., 286, 2021, 112226.

7. T. Bi, Zh. Du, Sh. Chen, H. He, X. Shen, Y, Fu, Preparation of flower-like ZnO photocatalyst with oxygen vacancy to enhance the photocatalytic degradation of methyl orange, Appl. Surf. Sci., 614, 2023, 156240.

8. Z. Zaaboub, F.Hassen, L.Chaabane, H. Maaref, Photoluminescence and time resolved photoluminescence properties in as grown ZnO thin films prepared by DC reactive sputtering for optoelectronic devices, Microelectron. J., 114, 2021, 105153.

9. J. Ramos-Serrano, S. Alcantara-Iniesta, M. Acosta-Osorno, M. Calixto, Growth of highly c-axis oriented ZnO thin films by spray pyrolysis for piezoelectric applications, Mater. Sci. Semicond. Process., 144, 2022, 106585.

10. Y. Liu, Z. Zhu, Y. Cheng, B. Wei, Y. Cheng, Effect of electrodeposition temperature on the thin films of ZnO nanoparticles used for photocathodic protection of SS304, J. Electroanal. Chem., 881, 2021, 114945.

11. N. Vega, B. Straube, O. Marin-Ramirez, D. Comedi, Low temperature chemical vapor deposition as a sustainable method to obtain c-oriented and highly UV luminescent ZnO thin films, Mater. Lett., 333, 2023, 133684.

12. C. Teran, J. Calderon, H. Quiroz, A. Dussan, Optical properties and bipolar resistive switching of ZnO thin films deposited via DC magnetron sputtering, Chin. J. Phys., 74, 2021, 1-8.

13. M. Murthy, C. Sreelatha, G. Ravinder, S. Anusha, The effect of solution pH on the structural, surface morphological, and optical characteristics of ZnO thin films synthesized by the chemical bath deposition technique, Mater.today: Proceed., 54, 3, 2022, 602-607.

14. H. Shen, X. Shi, Z. Wang, Z. Hou, Ch. Xu, L. Duan, S. Zhao, H. Wu, Defects control and origins of blue and green emissions in sol-gel ZnO thin films, Vacuum, 202, 2022, 111201.

15. E. Daher, B. Riachi, J. Chamoun, Ch. Laberty-Robert, W. Hamd, New approach for designing wrinkled and porous ZnO thin films for photocatalytic applications, Colloid. Surf. A: Physochem. Eng. Asp., 658, 2023, 130628.

16. T. Kamal, M. Ul-Islam, S. Khan, A. Asiri, Adsorption and Photocatalyst Assisted Dye Removal and Bactericidal Performance of ZnO/Chitosan Coating Layer, Int. J. Biol. Macromol. 81, 2015, 584-590.

17. 17. A. Mragui, O. Zegaoui, J. Esteves da Silva, Elucidation of the Photocatalytic Degradation Mechanism of an Azo Dye under Visible Light in the Presence of Cobalt Doped TiO_2 Nanomaterials, Chemosphere, 266, 2021, 128931.

18. E. Baylan, O. Yildirim, Highly Efficient Photocatalytic Activity of Stable Manganese-Doped Zinc Oxide (Mn:ZnO) Nanofibers via Electrospinning Method, Mater. Sci. Semicond. Process., 103, 2019, 104621.

19. Y. Wang, J. Cheng, S. Yu, E. Alcocer, M. Shahid, Z. Wang, W. Pan, Synergistic Effect of N-Decorated and Mn^{2+} Doped ZnO Nanofibers with Enhanced Photocatalytic Activity, Sci. Rep., 6, 2016, 32711.

20. K. Qi, X. Xing, A. Zada, M. Li, Q. Wang, Y. Liu, H. Lin, G. Wang, Transition Metal Doped ZnO Nanoparticles with Enhanced Photocatalytic and Antibacterial Performances: Experimental and DFT Studies, Ceram. Int., 46, 2020, 1494-1502.

21. S. Senthilkumaar, K. Rajendran, S. Banerjee, T. Chini, V. Sengodan, Influence of Mn Doping on the Microstructure and Optical Property of ZnO, Mater. Sci. Semicond. Process., 11, 2008, 6-12.

22. J. Yang, L. Shi, L. Wang, S. Wei, Non-Radiative Carrier Recombination Enhanced by Two-Level Process: A First-Principles Study, Sci. Rep., 6, 2016, 21712.

23. A. El Mragui, I. Daou, O. Zegaoui, Influence of the Preparation Method and $ZnO/(ZnO + TiO_2)$ Weight Ratio on the Physicochemical and Photocatalytic Properties of $ZnO-TiO_2$ Nanomaterials, Catal. Today, 321-322, 2019, 41-51.

24. I. Daou, O. Zegaoui, A. Elghazouani, Physicochemical and Photocatalytic Properties of the ZnO Particles Synthesized by Two Different Methods Using Three

Different Precursors, C.R. Acad. Sci., Ser. IIc: Chim., 20, 2017, 47-54.

25. R. Nithya, S. Ragupathy, D. Sakthi, V. Arun, N. Kannadasan, A Study on Mn Doped ZnO Loaded on CSAC for the Photocatalytic Degradation of Brilliant Green Dye, Chem. Phys. Lett., 755, 2020, 137769.

26. P. Basnet, D. Samanta, T. Chanu, S. Chatterjee, Visible Light Facilitated Degradation of Alternate Dye Solutions by Highly Reusable Mn-ZnO Nano-Photocatalyst, J. Alloys Compd., 867, 2021, 158870.